FROM SINGLE-PULSE TO FULL-WAVEFORM AIRBORNE LASER SCANNERS: POTENTIAL AND PRACTICAL CHALLENGES

W. Wagner [a, *], A. Ullrich [b], T. Melzer [a], C. Briese [c], K. Kraus [c]

[a] Christian Doppler Laboratory for Spatial Data from Laser Scanning and Remote Sensing, Vienna University of Technology, Gusshausstrasse 27-29, 1040 Vienna, Austria - (ww, tm)@ipf.tuwien.ac.at
[b] Riegl Research GmbH, 3580 Horn, Austria - aullrich@riegl.co.at
[c] Institute of Photogrammetry and Remote Sensing, Vienna University of Technology, Gusshausstrasse 27-29, 1040 Vienna, Austria - (cb, kk)@ipf.tuwien.ac.at

KEY WORDS: Laser scanning, Digitisation, Retrieval, Vegetation, Accuracy, Automation

ABSTRACT:

Airborne laser scanning, often referred to as lidar or laser altimetry, is a remote sensing technique which measures the round-trip time of emitted laser pulses to determine the topography of the Earth's surface. While the first commercially available airborne laser scanners recorded only the time of one backscattered pulse, state-of-the-art systems measure first and last pulse; some are able to measure up to five pulses. This is because there may be several objects within the travel path of the laser pulse that generate multiple echoes. Pulse detection is then used to determine the location of these individual scatterers. In this paper we discuss the physical measurement process and explain the way how distributed targets (such as trees or inclined surfaces) transform the emitted pulse. It is further shown through theoretical experiments that different detectors may yield quite different height information, depending on the type of the target. For example, even in the simple case of a tilted roof (with a tilt angle of 45°) the range values obtained by using different detectors may vary by ~ 0.4 m for a laser footprint size of 1 m. Airborne laser scanner systems that digitise the full waveform of the backscattered pulse would give more control to the user in the interpretation process. It would e.g. be possible to pre-classify the acquired data with respect to the shape of the echoes, to use different detection methods depending on surface cover and the intended application, and to employ more physically-based retrieval methods.

1. INTRODUCTION

Airborne laser scanning is a rapidly growing technology which has initially been conceived for topographic mapping. Airborne laser scanners employ, with few exceptions, pulsed lasers that repetitively emit short infrared pulses towards the Earth's surface. Some of the energy is scattered back to the sensor where it is measured with an optical receiver. A timer measures the travelling time of the pulse from the laser scanner to the Earth's surface and back. Since the round-trip time is directly related to the distance of the sensor to the ground, the topography of the Earth's surface can be reconstructed.

One advantage of airborne laser scanning compared to classical photography is that laser scanners are not dependent on the sun as a source of illumination. Consequently, the interpretation of laser scanner data is not hampered by shadows caused by clouds or neighbouring objects. For example, laser scanner pulses may travel unimpeded back and forth along the same path through small openings in a forest canopy, providing information about the forest floor. In contrast, optical images provide information only about the illuminated top layers of the forest canopy, while lower canopy layers and the forest floor constitute a dark background.

Since 1960, when Theodore Maiman demonstrated that "light amplification by stimulated emission of radiation" (laser) is also possible in the infrared and optical part of the electromagnetic spectrum, lasers have been widely used for military intelligence and civil surveying. But it took more then thirty years before laser scanners were deployed on commercial airborne platforms for topographic mapping purposes. There are many reasons for the relatively late adoption of airborne laser scanner technology: Flood (2001) mentions as critical factors the increasing availability of commercial off-the shelf sensors in the mid-90s, advancements in the design and capabilities of the sensors themselves, and an increased awareness by end users and contracting agencies. Ackermann (1999) points out the importance of precise kinematic positioning of the airborne platform by differential GPS ("Global Positioning System") and inertial attitude determination by IMU ("Internal Measurement Unit") for accurate referencing to an external coordinate system. Finally, also the increasing computer power probably played an important role, given that a large amount of data is acquired during each laser scanner flight (0.1 - 10 points per square meter).

The development of airborne laser scanning has been largely technology driven (Ackermann, 1999), but advances in our understanding of the measurement process have quickly led to system improvements. The first commercially available airborne laser scanners recorded the time of one backscattered pulse. The recording of only one pulse is sufficient if there is only one target within the laser footprint. In this case the shape of the reflected pulse is "single mode" and straightforward to interpret. However, even for small laser footprints (0.2 - 2 m) there may be several objects within the travel path of the laser pulse that generate individual backscatter pulses. Therefore more

* Corresponding author

advanced laser scanners have been built which are capable of recording more than one pulse. State-of-the-art commercial laser scanners typically measure first and last pulse; some are able to measure up to five pulses. Still, the problem is that it is not always clear how to interpret these measurements for different targets, particularly if the detection methods for the determination of the trigger pulses are not known. Pragmatically, one may for example assume over forested terrain that the first pulse is associated with the top of canopy and the last pulse, with some probability, with the forest floor. However, due to the 3D structure of natural and artificial objects, the form of the received pulses may be quite complex. The number and timing of the recorded trigger-pulses are therefore critically dependent on the employed detection algorithms. Consequently, it appears to be the logical next step to employ laser scanners that are able to record the full-waveform. In fact, first commercial full-waveform laser scanner systems will become available in the near future.

Another, to a certain degree oppositional trend in laser scanner scanning, is the design of laser beams with smaller and smaller beam divergence (tendency to "single mode" signals). With this sensors the number of multiple returns per emitted pulse will decrease, due to the fact that a smaller surface patch is illuminated. Since the acquired information per beam decreases, classification of the data is only possible in relation to neighbouring echoes. An interesting aspect for the future system design may eventually be the combination of narrow (only one single return with high quality range information) and wide (recording the full-waveform information) beams in order to use the advantages of both techniques.

In order to exploit the potential of full-waveform digitising laser scanners, the physical measurement process must be well understood (Wagner et al., 2003). In this paper we shortly review the technical characteristics of laser scanning systems (Section 2) and discuss basic physical concepts that allow to understand the way how distributed targets (such as trees or inclined surfaces) transform the emitted pulse (Section 3). By taking simple examples, the implications of using different post-processing algorithms for the determination of trigger-pulse are demonstrated (Section 4). Finally, section 5 discusses some of the issues that need to be addressed by future research and development efforts in order to fully exploit full-waveform laser scanners.

2. LASER SCANNER SYSTEMS

All commercial airborne laser scanner systems measure the travelling time of short laser pulses (pulses are typically 5-10 ns long), but otherwise may vary significantly in their design. For example, some systems use rotating mirrors as deflection units, others glass fibres. The laser wavelength is typically in the range from 0.8 to 1.55 μm.

Figure 1 illustrates this distance measurement principle. An emitted laser scanner pulse (here we use for simplicity a square pulse) interacts with the earth's surface. This interaction leads, if the pulse illuminates a vertically elongated surface target, to a significant change of the shape of the pulse. The goal of the distance measurement system is the detection of a previously defined reference point (based on the emitted signal, e.g. the raising edge) in the reflected echo. For this task different detection methods (further details will be presented in section 4) can be used. In Figure 1 the use of a threshold operator is demonstrated. In this example two stop pulses are detected. The use of different detection methods can lead to different results especially in areas with more than one reflecting element within one laser spot (see Section 4.2).

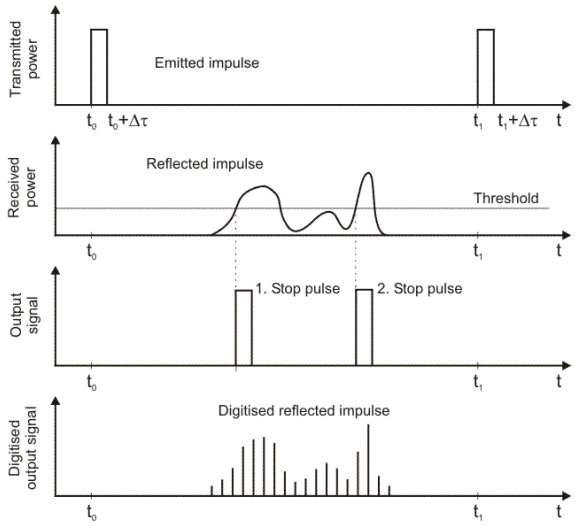

Figure 1. Emitted and received impulse. Commercial systems estimate the travel time of more than one stop impulses. Experimental systems digitise the whole waveform of the received echo with a certain sampling interval.

Current commercial system providers do not offer detailed information concerning their detection method, so that the end user has no information about the varying quality of the range measurements. Therefore the influence of the detection method on the finally computed models is presently unknown.

The US National Aeronautics and Space Administration (NASA) has already developed and operated waveform digitising airborne laser scanners for demonstrating the potential of this technique for vegetation mapping. For example, the airborne prototype LVIS (Laser Vegetation Imaging Sensor) employs a digitiser sampling rate of 500 Msamples per second (Blair et al., 1999). This corresponds to a range sampling interval of 0.3 m. Hofton and Blair (2002) write that this sampling interval is sufficient to reconstruct the shape of the pulse with a vertical resolution of about 0.03 m.

3. PHYSICAL PRINCIPLES

Laser scanning is a direct extension of conventional radar (radio detection and ranging) techniques to very short wavelengths. Whether laser scanning is referred to as lidar (light detection and ranging), laser altimetry, or laser radar, the same basic principles as in microwave radar technology apply (Jelalian, 1992). As a result, much of the terminology and concepts used in radar remote sensing can be directly transferred to laser scanning. In section 3.1 we introduce the radar equation, which is the fundamental model for describing the measurement process in terms of sensor and target characteristics. In section 3.2 it is shown that the form of the received pulse can mathematically be depicted by a convolution between the emitted pulse and the (effective) scattering cross-section of the Earth's surface.

3.1 Radar Equation

The intensity of the received laser pulse can be determined from the range equation, which describes the influences of sensor, target, and atmosphere (Jelalian, 1992):

$$P_r = \frac{P_t D_r^4}{4\pi R^4 \beta_t^2} \cdot \eta_{sys} \eta_{atm} \cdot \sigma \qquad (1)$$

where P_r = received signal power (watt)
P_t = transmitted signal power (watt)
D_r = diameter of receiver aperture (meter)
R = range from sensor to target (meter)
β = laser beamwidth (radian)
η_{sys} = system transmission factor
η_{atm} = atmospheric transmission factor
σ = target cross section (square meters)

The radar equation shows that the received power is a function of transmitter power, laser beamwidth, aperture size of the receiver, system losses, and atmospheric transmission. The properties of the target are described by a single quantity, the backscattering cross section.

The backscattering cross section is, as its name suggest, the effective area for collision of the laser beam and the target, taking into account the directionality and strength of the reflection (Jelalian, 1992). Therefore it has a unit of square meters. In the case of airborne laser scanning the wavelength is always much smaller than the size of the scattering elements (e.g. leaf, roof). Therefore, the effective area for collision is simply the size of the projected area of the scatterer. The magnitude and directionality of the reflected energy depends strongly on the surface properties of the target and its orientation with respect to the incoming beam.

3.2 Pulse Form

Models which are capable of simulating the waveform from different targets are already available. For example, Sun and Ranson (2000) present a model for forest canopies which assumes that laser scanners are working on a hot spot condition (because the light source and detector are at the same point). Here we build upon the radar equation, noting that in the way as it is written in equation (1) it only applies for point scatterers or non-tilted surfaces. In case of distributed targets, where scattering of the incoming laser beam takes place within the range interval $[R_1, R_2]$, the return-signal strength is the superposition of echoes from portions of the target at different ranges (Ulaby et al., 1981). Mathematically, this can be expressed by an integral:

$$P_r(t) = \int_{R_1}^{R_2} \frac{D_r^2}{4\pi R^4 \beta_t^2} \cdot \eta_{SYS} \eta_{ATM} \cdot P_t\left(t - \frac{2R}{v_g}\right) \cdot \sigma(R) dR \qquad (2)$$

where t is the time, v_g is the group velocity of the laser pulse, and $\sigma(R)dR$ is the differential backscattering cross section $d\sigma$ in the interval dR (Wagner et al., 2004). The group velocity v_g for optical and near-infrared radiation in dry air differs from the speed of light in vacuum by at most 0.03 % (Rees, 2001), so here we use $v_g \approx 3 \cdot 10^8$ m·s^{-1}. The term $2R/v_g$ in the brackets is the round trip time.

It must be considered that at range R some scattering elements may be shaded by objects situated above this range, i.e. in the interval $[R_1, R]$. Since these shaded areas do not contribute to the return signal, $d\sigma$ represents an "effective" or "apparent" cross section that represents only illuminated scatterers in dR. As an example, lets us consider the ground surface beneath a tree. If 90 % of the ground surface is shaded by leaves and branches, then the "effective" cross section of the ground is 10 % of its actual cross section.

In the next section we will study the impact of different pulse detection methods on the distance measurements. For this purpose it is sufficient, in a first step, to focus solely on the waveform of the return pulse. In more advanced studies also the different parameters which modulate the signal strength should be considered.

4. IMPACTS OF PULSE DETECTION

4.1 Detection Methods

Pulse detection is applied on the backscattered waveform. The task of the detector is to derive from the continuous waveform discrete, time-stamped *trigger-pulses*, which encode the position of the individual targets, thus allowing to compute the distance between the scanner system and the generator of the return pulses, i.e., the illuminated objects. Since the details of detection methods applied by commercial laser scanner systems are currently not known, we will consider here a number of standard detection methods: *threshold*, *centre of gravity*, *maximum*, *zero crossing* of the second derivative, and *constant fraction*.

The most basic technique for pulse detection is to trigger a pulse whenever the rising edge of the signal exceeds a given *threshold* (Figure 1); although conceptually simple and easy to implement, this approach suffers from a serious drawback: the position of the triggered pulse (and thus the accuracy of any distance measurements derived from it) is rather sensitive to the amplitude and width of the signal. The same holds for the *centre of gravity* when computed over all points above a fixed threshold. More sophisticated schemes are based on finite differences respectively numerical derivatives – e.g., the detection of local *maxima* or the *zero crossings* of the second derivative – or, more generally, the zero-crossings of a linear combination of time-shifted versions of the signal. An example of the latter approach is the *constant fraction* discriminator, which determines the zero crossings of the difference between an attenuated and a time delayed version of the signal. *Maximum*, *zero crossing*, and *constant fraction* are invariant with respect to amplitude variations and, to some degree, also changes in pulse width. In practice, these detectors should only trigger for signal amplitudes above a given threshold (this "internal" threshold is not to be confused with the *threshold* detector) in order to suppress false positives, i.e. spurious trigger-pulses due to noise. This is especially true for operators based on higher order derivatives like *zero crossing*, which are known to be rather noise-sensitive.

Figure 2 illustrates the trigger-pulses generated by the five detectors discussed above for the case of a single mode return signal from rough terrain, assuming a Gaussian differential

scattering cross section $d\sigma$ with a standard deviation of 0.05 m, shown in Figure 2 at a distance of 9 m. The emitted pulse is in our example a long-tailed "10ns" *Q-switched pulse*, which bears only a faint resemblance to an idealised rectangular pulse. The backscattered waveform, which is obtained as convolution of the emitted signal with the assumed terrain cross section, is – due to the narrow shape of the cross section in this example – basically a time-delayed and slightly widened version of the emitted pulse.

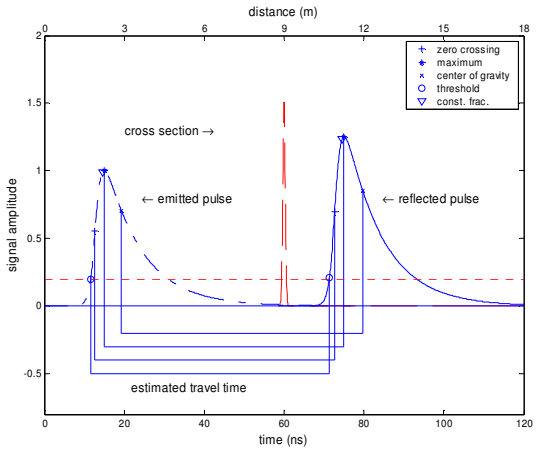

Figure 2. Emitted pulse and single-mode return signal for a Gaussian cross section. Also shown are the time differences between corresponding trigger-pulses derived from the emitted and reflected signal. The dashed horizontal line at y = 0.2 indicates the threshold level used by the *threshold* and *centre of gravity* methods.

In order to determine the precise distance of an object, the detected pulse in the reflected signal must be related to the emitted pulse; here, we assume this is done by applying the same pulse detector to both signals, although other approaches are possible. The measured time differences (and thus distances) between corresponding trigger-pulses indicated in Figure 2 – the estimated travel time - should be 60 ns (9 m) for all five detectors; however, even in this quite benign case, only the three "difference"-based detectors give correct results (see Table 1); for example, the estimated travel time for the *threshold* method is 59.7 ns, resulting in a range error of (60 – 59.7)×0.3/2 = 0.045 m.

4.2 Experiments

In this subsection, we will highlight the properties of the different pulse detectors by applying them to several simulated waveforms; quantitative results for all experiments are given in Table 1. The first experiment, shown in Figure 3, assumes wheat crops on rough ground. The differential scattering cross section of wheat is assumed to consist of two peaks, the first relating to the wheat and the second to the underlying ground. Since the scattering centres of wheat and the ground are relatively close (only 0.6 m apart), their vertical profiles are merged into a unimodal waveform by the convolution (Figure 3, bottom). As can be seen from Table 1, the best results are obtained by the *zero crossing* method; it is also the only detector that generates two trigger-pulses and correctly resolves (discriminates) the waveform into ground and vegetation components. However, as noted before, *zero crossing* is sensitive to noise.

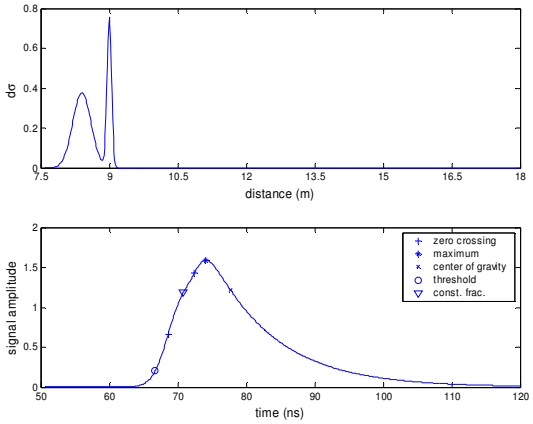

Figure 3. Return pulse of a wheat field. Top: Assumed effective scattering cross section of a wheat field (crops on rough ground). Bottom: Reflected signal and derived trigger-pulses.

Fig.	object	dist.	zc	max	thr	cog	cf
2	ground	9.0	0.000	0.000	0.045	-0.060	0.000
3	crops	8.4	0.015	-	0.135	-	-0.030
	ground	9.0	0.045	0.150	-	0.240	-
4	branch1	8.0	0.019	-0.131	-0.161	-0.101	0.049
	tree	10.0	-1.250	-	-	-	-
	branch 2	13.0	0.026	-0.035	-0.049	0.446	
	bush	20.0	0.110	-	-	-0.371	0.230
	ground	21.0	0.000	0.060	-0.210	-	0.135
5	roof	9.0	0.075	-0.150	0.240	-0.135	0.015

Table 1. True object distances and range errors (in m) for the different detectors. The positional errors are obtained by multiplying the difference between true and estimated travel time by 0.3/2, e.g., 1 ns corresponds to 0.15 m. Detection methods: zc = *zero crossing*, max = *maximum*, thr = *threshold*, cog = *centre of gravity*, cf = *constant fraction*.

In the second experiment, shown in Figure 4, we assume a somewhat more complex scenario: the laser beam passes through a treetop with two prominent branches, then through low vegetation (bushes) and finally reaches the ground. Again, *zero crossing* detects all five objects (see Table 1); however, the error for the treetop volume is rather high due its wide spread and the interference of the branches.

Note that the trigger-pulses derived by *center of gravity* tend to lie between those derived by *zero crossing* and *maximum* (nearer to *zero crossing* for slow edges and nearer to *maximum* for fast, steep edges). It is also interesting to note that in this example both *constant fraction* and *zero crossing* are able to distinguish between low vegetation and ground, although their respective cross sections are still rather close (1 m).

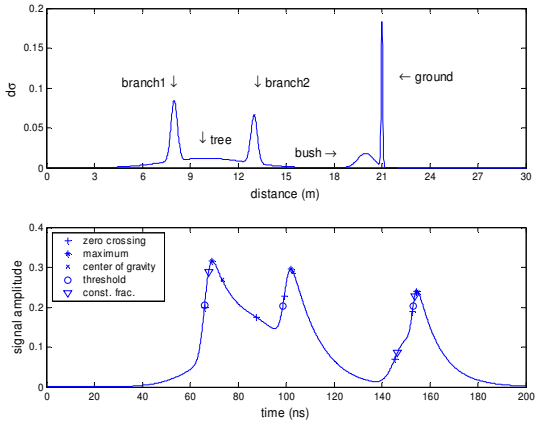

Figure 4. Return pulse of a tree. Top: Assumed effective scattering cross section of tree, including branches, low vegetation and ground. Bottom: Reflected signal and derived trigger-pulses.

In the third and final experiment, we investigate the detector performance on a waveform resulting from the interaction of the laser beam with a tilted roof, assuming a tilt angle of 45° and pulse diameter of 1 m. As can be seen from Figure 5, top, the scattering cross section has the form of a half-ellipse (the effect of the tilt is to "stretch" the circular footprint into an ellipse; the cross section is thus proportional to the width of the ellipse - measured along the minor axis – as function of height.) Here, the best result is obtained by *constant fraction*. This example demonstrates, in particular, that *zero crossing*, although it excels at resolving narrow, sharply peaked components of the cross section, performs less well in the case of broad, plateau-like maxima (such a constellation will, in general, lead to premature triggering). Remarkable to note is that even in this simple case the range values obtained by using different detectors may vary by ~ 0.4 m (*max* compared to *centre of gravity*), which is a large number given that the laser footprint is 1 m.

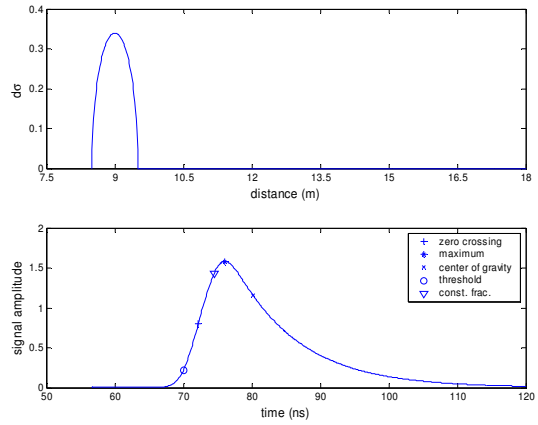

Figure 5. Return pulse of tilted roof. Top: Assumed effective scattering cross section of tilted roof. Bottom: Reflected signal and derived trigger pulses.

4.3 Discussion

As illustrated by the above experiments, there is no such thing as a single best detector; rather, the relative performance of the detectors depends on several factors, such as the characteristics of the effective scattering cross section, object distance and noise level. For example, although *zero crossing* yields excellent range resolution (discrimination between nearby objects) and range accuracy under ideal conditions, it is susceptible to noise (spurious trigger pulses) and slow gradients (decrease in accuracy). *Threshold* may yield good accuracy for a single object at a given distance, but poor range estimates (or no trigger-pulse at all) if the amplitude of the back-scattered pulse changes (i.e., due to an increase in object-sensor distance or absorption/reflection of pulse energy by other objects). *Maximum*, while not as accurate as *zero crossing,* gives reasonably good results and can be expected to be more tolerant against noise than *zero crossing*. *Constant fraction* seems to be a good compromise between *zero crossing* and *maximum.*

The experiments presented in this section have mainly qualitative character and are intended to illustrate the dependency of the backscattered waveform on the scattering cross sections of the illuminated objects, and to highlight the respective strengths and weaknesses of various approaches to pulse detection. Clearly, more elaborate experiments, both on synthetic and real world data, will have to be conducted in order to gain a better understanding of the physical principles underlying waveform generation as well as the effects of noise and scanner characteristics on detection performance.

5. OUTLOOK

In anticipation of the potential of full-waveform lasers for vegetation mapping experimental systems have already been built and tested by NASA (Blair et al., 1999). Soon, also commercial full-waveform systems will become available.

RIEGL Laser Measurement Systems GmbH will soon offer a 2D laser scanner for airborne applications (model *RIEGL* LMS-Q560) with an optional data logger capability for recording the digitised waveforms of both the transmitted laser pulse and the echo signal (Riegl 2004). Laser pulse repetition rate is 50 kHz and maximum range is typically 1500 m on targets with 80% reflectivity. Sampling of the echo signal is carried out simultaneously in two 8bit channels in order to cover a dynamic range of about 40 dB optically. Sampling rate is 1GSamples/sec for each channel. Samples within a configurable range gate centred around detected targets are stored on redundant large volume drives together with time stamp and scan angle data. The maximum number of targets and the number of samples per target to be logged can be defined by the user within limits defined by the writing speed of the data logger and its capacity limitation. Single target measurement accuracy is about 2 cm (1 sigma value).

As for each laser measurement also a fraction of the transmitted laser pulse is sampled, the pulse shape of the transmitter pulse can be evaluated from numerous measurements with high resolution as shown in Figure 6. Pulse width of the sampled pulse is about 4.5 ns (at 50% maximum amplitude) which is the result of the convolution of the laser pulse and the pulse response of the receiver. This measured pulse shape can be used advantageously as the basis for the analysis of the echo signal of complex targets.

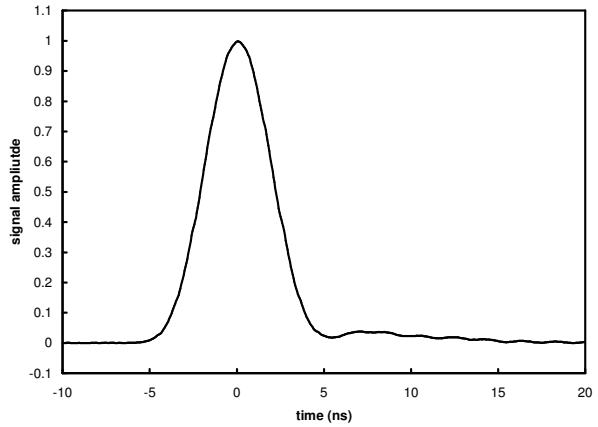

Figure 6. High-resolution sampled transmitter pulse of RIEGL LMS-Q560. Temporal resolution 50 ps, calculated from samples on 2000 consecutive transmitter pulses.

Figure 7 shows an example of the echo signal obtained on a coniferous tree at a distance of about 260 m. Three separate targets can be identified which can be attributed to different twigs.

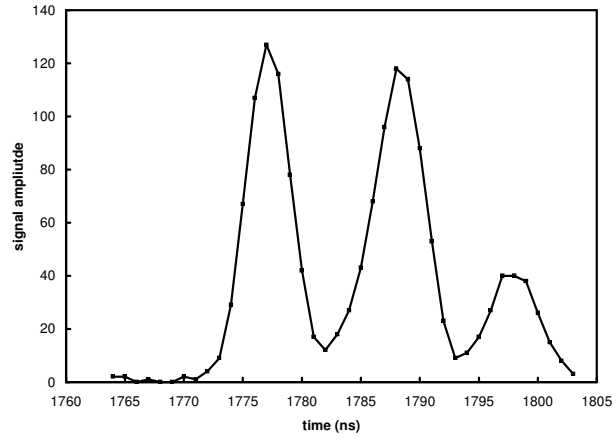

Figure 7. Example of received echo signal of the RIEGL LMS-Q560 on a coniferous tree in about 260 m distance showing three distinct targets with distance differences of about 1.5 m.

Digitisation and recording of part of or even the full return signal by commercial full-waveform airborne laser scanners like the one sketched above will provide additional information about the structure of the illuminated surface. This offers the option of classifying the acquired data based on the shape of the echo (e.g. separating narrow return echoes from horizontal terrain surfaces from wide echoes with more than one peak in wooded areas). Another important advantage is that the detection of the stop (trigger) pulses can be applied after data capturing, thus allowing to use different detection methods or even a combination of methods in order to extract the most interesting information for a specific application. An end user who wants to model the vegetation structure has different requirements on the detection method than a user who is interested in terrain modelling.

Unfortunately, current systems do not provide any information about the echo detection method and offer no quality feedback, even though this information could be very useful for further modelling steps. In contrast, future systems with full-waveform recording capability will allow to apply one of several pulse detection methods after data acquisition. By local analysis of the backscattered signal, it should also be possible to determine quality parameters for a given range measurement, which can be used as a direct input into further processing steps.

It appears that full-wave systems will much enhance our capability to map natural and artificial objects, but this comes at a cost: Instead of having one or a few trigger pulses the whole discrete signal must be stored. Major research and development efforts will be needed in order to develop algorithms and software that can efficiently transform the recorded waveform clouds into geo-spatial data sets.

ACKNOWLEDGEMENTS

The contribution of Christian Briese was supported by the Austrian Science Foundation (FWF) under grant no. P-15789.

REFERENCES

Ackermann, F., 1999. Airborne laser scanning - present status and future expectations. *ISPRS Journal of Photogrammetry & Remote Sensing*, 54, pp. 64-67.

Blair, J. B., D. L. Rabine, and M. A. Hofton, 1999. The Laser Vegetation Imaging Sensor: a medium-altitude, digitisation-only, airborne laser altimeter for mapping vegetation and topography. *ISPRS Journal of Photogrammetry & Remote Sensing*, 54, pp. 115-122.

Flood, M., 2001. Laser altimetry: From science to commercial lidar mapping. *Photogrammetric Engineering & Remote Sensing*, 67(11), pp. 1209-1217.

Hofton , M. A., and J. B. Blair, 2002. Laser altimeter return pulse correlation: a method for detecting surface topographic change, *Journal of Geodynamics*, 34, 477-489.

Jelalian, A. V., 1992. *Laser radar systems*. Artech House, Boston and London, 292p.

Rees, W. G., 2001. Physical principles of remote sensing. Cambridge University Press, Cambridge, 343p.

Riegl Laser Measurement Systems, 2004. Website www.riegl.com.

Sun, Q., and K. J. Ranson, 2000. Modeling lidar returns from forest canopies. *IEEE Transactions on Geoscience and Remote Sensing*, 38(6), pp. 2617-2626.

Ulaby, F. T., R. K. Moore, A. K. Fung, 1981. *Microwave remote sensing: Active and passive*. Volume I, Artech House, Noorwood, 456p.

Wagner, W., A. Ullrich, and C. Briese, 2003. Der Laserstrahl und seine Interaktion mit der Erdoberfläche. *Österreichische Zeitschrift für Vermessung & Geoinformation*, VGI 4/2003, pp. 223 - 235.